

# Cluster Aggregated GAN (CAG): A Cluster-Based Hybrid Model for Appliance Pattern Generation

Zikun Guo<sup>a</sup>, Adeyinka.P. Adedigba<sup>a</sup> and Rammohan Mallipeddi<sup>a,\*</sup>

<sup>a</sup>Department of Artificial Intelligence, School of Electronics Engineering, Kyungpook National University, 80 Daehak-ro, Buk-gu, Daegu, 41544, Republic of Korea

## ARTICLE INFO

### Keywords:

Generative adversarial networks  
non intrusive load monitoring  
Pattern generation  
Clustering  
LSTM

## ABSTRACT

Synthetic appliance data are essential for developing non-intrusive load monitoring algorithms and enabling privacy preserving energy research, yet the scarcity of labeled datasets remains a significant barrier. Recent GAN-based methods have demonstrated the feasibility of synthesizing load patterns, but most existing approaches treat all devices uniformly within a single model, neglecting the behavioral differences between intermittent and continuous appliances and resulting in unstable training and limited output fidelity. To address these limitations, we propose the Cluster Aggregated GAN framework, a hybrid generative approach that routes each appliance to a specialized branch based on its behavioral characteristics. For intermittent appliances, a clustering module groups similar activation patterns and allocates dedicated generators for each cluster, ensuring that both common and rare operational modes receive adequate modeling capacity. Continuous appliances follow a separate branch that employs an LSTM-based generator to capture gradual temporal evolution while maintaining training stability through sequence compression. Extensive experiments on the UVIC smart plug dataset demonstrate that the proposed framework consistently outperforms baseline methods across metrics measuring realism, diversity, and training stability, and that integrating clustering as an active generative component substantially improves both interpretability and scalability. These findings establish the proposed framework as an effective approach for synthetic load generation in non-intrusive load monitoring research.

## 1. Introduction

The growing deployment of smart meters and intelligent energy management systems has created an increasing demand for appliance level power consumption data. Such data serve multiple purposes in modern energy research: enabling the development of non intrusive load monitoring algorithms, supporting the stress testing of energy analytics pipelines, and facilitating privacy preserving data sharing scenarios [23]. However, acquiring sufficient quantities of real appliance data remains challenging. The collection process requires installing dedicated measurement equipment, obtaining user consent, and manually labeling individual device activations. These requirements make data collection resource demanding and potentially invasive to user privacy, establishing data scarcity as a persistent limitation in NILM research [18]. Given these constraints, generating realistic synthetic appliance data has emerged as a compelling alternative [10].

Despite considerable progress in generative modeling, producing realistic appliance load data remains challenging due to the fundamental heterogeneity of device behaviors. This heterogeneity manifests along two primary dimensions. First, intermittent devices such as laptops, refrigerators, and microwave ovens operate through discrete activation events. They exhibit rapid state transitions, frequent mode switching, and sharp transients with variable duty cycles. Second, continuous devices such as displays, printers in standby mode, and charging equipment maintain relatively stable power draws over extended periods. Their consumption trajectories evolve gradually without abrupt transitions. A single generative model trained on mixed data struggles to capture both regimes effectively, as their statistical properties and temporal structures differ substantially.

Recent advances in generative adversarial networks have demonstrated the feasibility of synthesizing appliance load patterns at scale [27]. These approaches based on GAN learn to produce consumption sequences that resemble real measurements in aggregate statistics. However, existing methods typically treat all appliances uniformly without

\*Corresponding author

Email addresses: gzk798412226@gmail.com (Z. Guo); yinkpeace@gmail.com (Adeyinka.P. Adedigba); mallipeddi.ram@gmail.com (R. Mallipeddi)

ORCID(s):

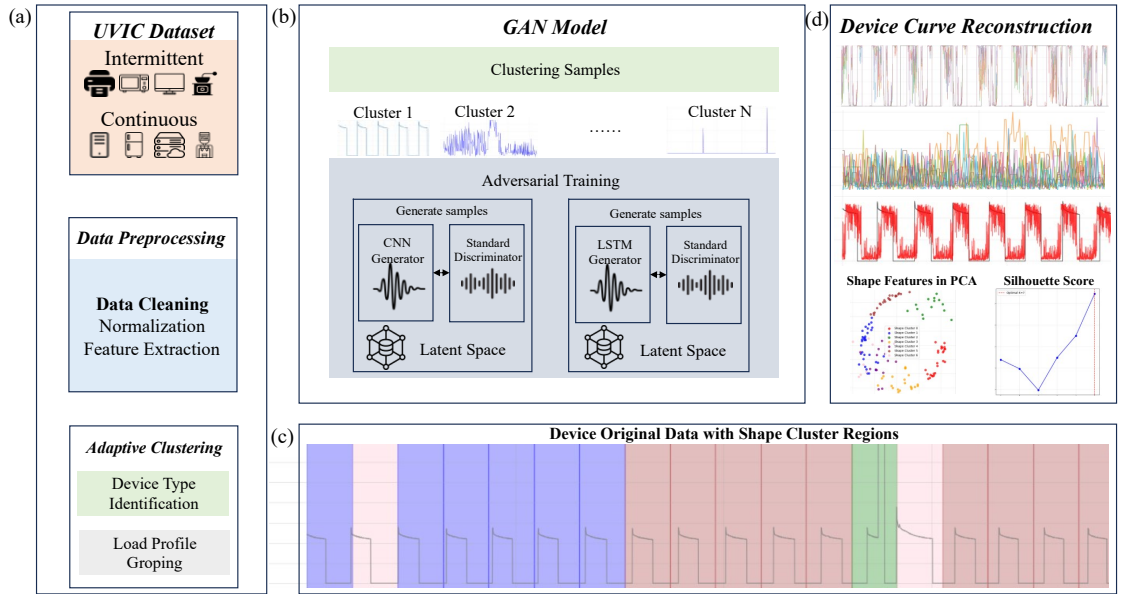


**Figure 1:** Overall workflow of the proposed Cluster Aggregated GAN framework for appliance load generation. Appliance traces are routed into intermittent or continuous branches by a lightweight classifier. Intermittent streams are clustered into patterns and modeled by dedicated CNN based generators for each cluster. Continuous streams are modeled by an LSTM based generator. A shared discriminator enforces realism across branches, and generated segments are merged into full device profiles.

explicitly accounting for the distinction between intermittent and continuous behaviors. This uniform treatment limits their capacity to reproduce the full diversity of load profiles observed in real households and reduces the utility of generated data for downstream applications.

The limitations of current approaches reveal three research gaps. First, appliance behavior spans multiple temporal scales and waveform characteristics. Within a single household, brief activation bursts, repeating cycles, and extended stable periods coexist. Capturing this diversity requires adaptive modeling strategies rather than uniform treatment. Second, existing generators tend to learn dominant patterns while failing to reproduce rare but important operational modes. This bias results in narrow output coverage and limits interpretability. Third, training stability becomes problematic when a single discriminator must evaluate fundamentally different behavioral types. Conflicting objectives when judging both smooth trajectories and sharp spikes often lead to mode collapse.

To address these challenges, we introduce the Cluster Aggregated GAN framework, referred to as CAG. The central idea behind CAG is to align the generative process with the inherent structure of appliance behaviors through two complementary mechanisms, namely behavioral routing and pattern aggregation. Rather than forcing a single model to learn all behavioral variations simultaneously, CAG decomposes the generation task according to device characteristics and operational patterns.

The framework operates as follows. A lightweight classifier routes each appliance trace to one of two specialized branches. Intermittent devices undergo pattern clustering, which groups similar operational modes and assigns dedicated generators to each cluster. This ensures that rare patterns receive adequate modeling capacity. Continuous devices follow a separate branch designed for sequential modeling of gradually evolving trajectories. A shared discriminator enforces consistent realism standards across both branches.

This design separates the modeling of activation timing from consumption morphology. Intermittent appliances benefit from pattern based generation that captures operational diversity, while continuous appliances benefit from sequence modeling that preserves smooth temporal evolution. The modular structure also improves interpretability, as each component corresponds to a specific aspect of appliance behavior. Figure 1 illustrates the overall workflow.

The contributions of this paper are threefold. First, we propose an automatic behavioral routing mechanism that distinguishes intermittent from continuous appliance behaviors based on activation statistics. This routing enables the

framework to steer each device toward a generative path suited to its operational characteristics, avoiding the limitations of uniform treatment. Second, we introduce a cluster based generative architecture that allocates dedicated modeling capacity to distinct behavioral patterns within the intermittent category. This design improves the coverage of rare operational modes and enhances the interpretability of the generation process by establishing explicit correspondences between model components and appliance behaviors. The architecture simultaneously maintains a streamlined path for continuous appliances, ensuring computational efficiency. Third, we conduct extensive experiments on a real smart socket dataset to validate the effectiveness of CAG. The results demonstrate that CAG generates appliance load data that faithfully capture the distinct characteristics of both intermittent and continuous devices. Compared to baseline methods, CAG achieves improved diversity in reproducing rare patterns and better alignment with real usage distributions as measured by downstream evaluation metrics.

## 2. Related Work

Time series data generation spans finance [19], medical monitoring [2, 12, 32, 40], IoT [6], and smart grids, where realistic synthetic data mitigates privacy, availability, and labeling limitations. Within NILM, early surveys and benchmarks stressed the scarcity of appliance traces and the need for reproducible datasets [5, 24]. Recent advances therefore emphasize privacy preserving synthesis using GANs with secure aggregation or decentralized updates [1, 37]. High frequency NILM datasets such as HiFakes explore synthetic data for diagnostics and cross dataset generalization [23], while simulators and digital twins provide controllable device waveforms [9, 21, 26]. Collectively, these efforts motivate appliance based generative modeling that balances fidelity, privacy, and scalability.

### 2.1. Generative Modeling for Time Series Data

Generic GAN based synthesizers treat appliance signals as a single distribution modeled by unified generators and discriminators. Foundational work established adversarial training principles and conditional variants but still relied on monolithic pipelines [8, 14, 30]. Early NILM GANs such as TraceGAN [18] and RLP-GAN [27] demonstrated that standard architectures could capture coarse appliance signatures, and follow up studies introduced device level tuning or adaptive weighting [13, 29]. Nevertheless, uniform generators often collapse rare patterns, fail to separate intermittent from continuous loads, and provide limited support for incorporating operational priors.

### 2.2. Clustering generative modeling

Cluster integrated approaches instead decompose the appliance space before generation. AMBAL aggregates load segments to model heterogeneous appliance behaviors [7], while SmartSim [9], SynD [26], and HYDROSAFE [22] rely on simulator orchestrated clusters to instantiate realistic schedules. Transformer based designs such as the cluster aggregated transformer [15] and IDS Extraction [17] exploit clustering to reduce complexity for long sequences, and ClusterGAN [31] objectives embed latent clustering directly in the adversarial training loop. Metadata GANs [28] and industrial digital twins [21] extend this idea to condition on contextual attributes, with NILMTK [5] providing the benchmarking infrastructure to evaluate clustered outputs. Despite their benefits, most methods keep clustering as a static preprocessing stage and do not adapt generator capacity to pattern complexity.

### 2.3. GAN architectures for time series

Architecture specialized methods such as Dynamic Tanh Transformer [16], tailor model classes to the temporal structure of appliance data. LSTM based GANs, including ALGAN [4], RCGAN [11], and other recurrent conditional variants, capture long range dependencies [39] but incur heavy training costs. CNN driven designs such as ConvTimeGAN [20] and TSGAN [34] emphasize local pattern encoding, whereas WaveGAN [38] generators model raw waveform continuity. Stability enhancements via WGAN critics [3] and auxiliary classifiers [33] reduce mode collapse, and hybrid generative paradigms like VAEs [25] or Transformer based NILM models [35, 36] broaden the inductive bias spectrum. However, these architectures largely ignore appliance heterogeneity, typically applying identical networks to diverse appliance types regardless of the operational characteristics.

Our CAG framework addresses these limitations by coupling adaptive device routing with shape based segment clustering and hybrid adversarial learning. Rather than treating clustering as auxiliary metadata, we bind it to generator selection so that convolutional pattern GANs focus on sporadic, intermittent loads while LSTM based sequence GANs model smooth, continuous appliances. Conditional guidance and discriminator specialization allow CAG to balance privacy needs with fidelity gains, inheriting the benefits of label guided GANs [30] without reverting to monolithic

generators. This integrated design improves pattern fidelity, stabilizes long duration training, and yields balanced behavioral coverage, establishing a pathway toward privacy conscious, appliance aware synthetic load generation for NILM analytics.

### 3. Method

#### 3.1. Overall Architecture

The core idea of CAG is to align the generative process with the behavioral heterogeneity of appliances through a structured pipeline that mirrors the intrinsic characteristics of real world device operations. As illustrated in Figure 2, the framework consists of four integrated stages: (i) dataset preparation, (ii) device classification, (iii) cluster aggregation for intermittent devices, and (iv) adversarial training with branch specific generators and a shared discriminator. The motivation behind this architecture stems from a fundamental observation in real household energy data: different appliances exhibit fundamentally different consumption signatures that cannot be effectively captured by a single generative model. Algorithm 1 outlines the pipeline.

#### 3.2. Device Classification

The first step in CAG is to route each appliance trace to an appropriate generative branch based on its behavioral characteristics. We formalize this process using the UVIC dataset of appliance power traces, which contains diverse real world consumption patterns from residential and office environments.

**Notation and Data Representation.** For an appliance with raw time series  $x_{1:T} \in \mathbb{R}^T$ , where  $T$  denotes the total number of samples, we form fixed length segments by non overlapping slicing:  $\{s^{(j)} \in \mathbb{R}^L\}_{j=1}^N$ , where  $L$  is the segment length and  $N = \lfloor T/L \rfloor$  is the number of segments. This segmentation serves multiple purposes: it creates training samples of uniform length required by neural networks, enables parallel processing of independent segments, and captures localized behavioral patterns that may vary over time. Let  $\Delta x_t = x_t - x_{t-1}$  denote the first order difference that approximates the instantaneous rate of change and  $\mathbb{1}[\cdot]$  the indicator function.

**Classification Features.** The classification relies on three lightweight statistics computed directly from the raw series  $x_{1:T}$ :

$$\begin{aligned} R_0 &:= \mathbb{1}[x_1 = \dots = x_{\min\{T_0, T\}} = 0], \\ p_{\text{nz}} &:= \frac{1}{T} \sum_{t=1}^T \mathbb{1}[x_t \neq 0], \\ \sigma_{\Delta}^2 &:= \frac{1}{T-1} \sum_{t=2}^T (\tilde{\Delta}x_t - \overline{\tilde{\Delta}x})^2, \end{aligned} \quad (1)$$

where  $\tilde{\Delta}x_t$  denotes the smoothed derivative obtained by applying a 7 point moving average filter before computing finite differences, and  $\overline{\tilde{\Delta}x}$  is its empirical mean.

The three features capture complementary aspects:  $R_0$  detects initial inactivity (continuous devices often start active),  $p_{\text{nz}}$  measures power occupancy (high for continuous, low for intermittent), and  $\sigma_{\Delta}^2$  quantifies temporal volatility after smoothing (low for gradual changes, high for frequent switching).

**Routing Rule.** The hyperparameters governing the classification are:  $T_0 \in \mathbb{N}$  (prefix length for detecting initial zero intervals),  $\rho \in (0, 1)$  (nonzero occupancy threshold), and  $\tau > 0$  (smoothed derivative variance threshold). Based on empirical analysis of the UVIC dataset, we set  $T_0 = 100$ ,  $\rho = 0.7$ , and  $\tau = 0.1$ . The routing decision follows:

$$\text{continuous if } R_0 = 1 \text{ or } (p_{\text{nz}} > \rho \wedge \sigma_{\Delta}^2 < \tau), \quad \text{else intermittent.} \quad (2)$$

This rule captures the intuition that continuous devices either start active or maintain high occupancy with low temporal variability, while intermittent devices exhibit sparse activations with high derivative variance. The classifier does not rely on device type labels and can be applied to new traces without retraining.

#### 3.3. Intermittent Device Generation

Intermittent devices present a unique challenge for generative modeling: their consumption patterns are inherently multimodal, comprising distinct operational states and usage scenarios. A single microwave, for instance, may exhibit

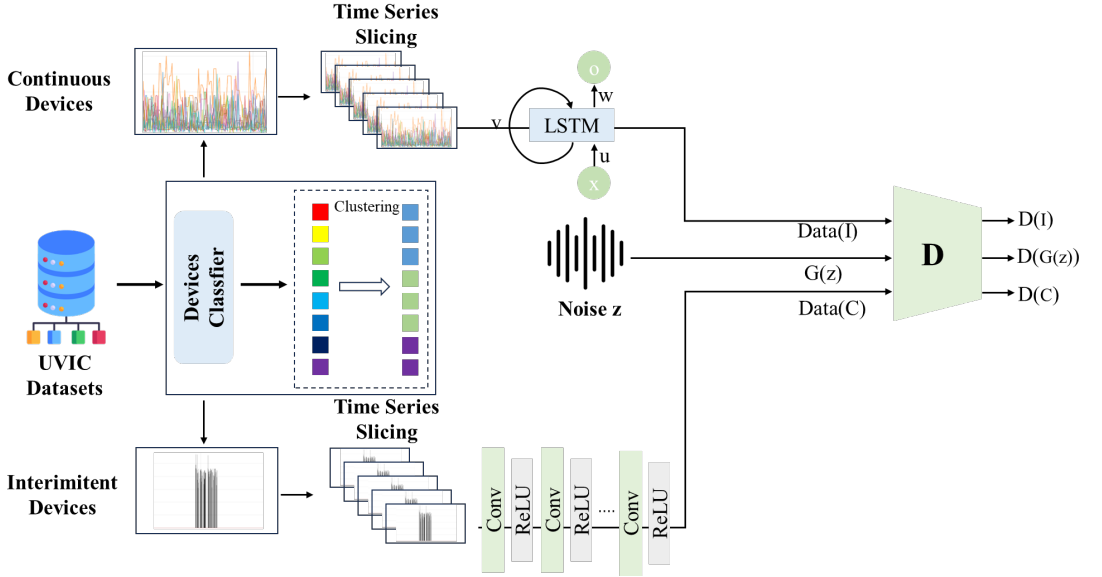


**Figure 2:** Cluster Aggregation GAN (CAG) overview. UVIC traces are routed by a lightweight classifier into intermittent and continuous devices. Intermittent streams are segmented, clustered, and generated via CNN based GANs assigned to each cluster. Continuous devices are downsampled and modeled by an LSTM based GAN. A shared discriminator  $D$  judges realism for all branches, promoting consistency across heterogeneous appliance behaviors.

different power profiles for defrosting (low power, long duration), reheating (medium power, variable duration), and cooking (high power, short duration). Rather than forcing a single generator to learn this complex mixture, CAG decomposes the problem through pattern clustering.

**Segment Normalization.** Before clustering, each segment  $s \in \mathbb{R}^L$  is normalized to remove scale differences and focus on shape characteristics:

$$\tilde{s} = \frac{s - \mu}{\sigma}, \quad (3)$$

where  $\mu$  and  $\sigma$  are the segment mean and standard deviation. This normalization removes scale differences, allowing clustering to group segments by morphological shape rather than absolute power levels.

**Feature Extraction.** Each normalized segment is transformed into a feature vector  $\phi : \mathbb{R}^L \rightarrow \mathbb{R}^d$  comprising: (i) statistical moments ( $\mu$ ,  $\sigma$ , skewness, kurtosis), (ii) trend coefficient  $\beta = \text{cov}(t, \tilde{s}) / \text{var}(t)$ , (iii) dominant frequency  $f^*$  from DFT magnitude, (iv) morphological counts (peaks, valleys), (v) roughness  $\text{var}(\Delta \tilde{s})$  and energy  $\|\tilde{s}\|_2^2$ , and (vi) 20 uniformly spaced shape samples. This multi-aspect representation enables clustering based on both statistical properties and temporal structure.

**K-Means Clustering.** After feature extraction, all features are standardized (z-scores) across segments to ensure equal weighting. The segments are then partitioned into  $K$  clusters using the k-means algorithm:

$$\min_{\{c^{(j)}\}, \{\mu^{(k)}\}} \sum_{j=1}^N \left\| \phi(s^{(j)}) - \mu^{(c^{(j)})} \right\|^2, \quad c^{(j)} \in \{1, \dots, K\}, \quad (4)$$

where  $c^{(j)}$  is the cluster assignment of segment  $j$  and  $\mu^{(k)}$  is the centroid of cluster  $k$ . This objective minimizes the total variance within each cluster, ensuring that segments assigned to the same cluster are similar in the feature space.

**Optimal Cluster Selection.** The number of clusters  $K$  is selected automatically by maximizing the mean silhouette score, subject to an upper bound  $K \leq \kappa$ :

$$\bar{s}(K) = \frac{1}{N} \sum_{j=1}^N \frac{b(j) - a(j)}{\max\{a(j), b(j)\}}, \quad (5)$$

where  $a(j)$  is the mean distance from segment  $j$  to other segments in the same cluster (measuring cohesion), and  $b(j)$  is the minimum mean distance to segments in other clusters (measuring separation). The silhouette score ranges from  $-1$  to  $1$ , with higher values indicating well defined clusters. This data driven selection ensures that the number of generators matches the intrinsic complexity of each device. Devices with diverse usage patterns receive more clusters, while simpler devices receive fewer.

For cluster  $k$ , the segment dataset is  $\mathcal{D}^{(k)} = \{s^{(j)} : c^{(j)} = k\}$ . For diagnostics and visualization, we project normalized segments onto principal components of their shape samples and overlay silhouette curves to illustrate cluster separability and diversity, as shown in the lower panel of Figure 1.

**Per-Cluster GAN Training.** Each cluster dataset  $\mathcal{D}^{(k)}$  trains an independent lightweight fully connected GAN. Let  $G(\cdot; \theta) : \mathbb{R}^{d(z)} \rightarrow [-1, 1]^L$  map a latent vector  $z \sim \mathcal{N}(0, I)$  to a synthetic segment, with a tanh output layer to bound the outputs. The discriminator  $D(\cdot; \psi) : [-1, 1]^L \rightarrow (0, 1)$  is a sigmoid classifier distinguishing real from generated segments. Training data are normalized to the range  $[-1, 1]$  per cluster to match the generator output range.

The adversarial training follows the standard GAN formulation with logistic losses:

$$\mathcal{L}^{(D)} = \frac{1}{2} \mathbb{E}^{x \sim p^{\text{real}}} [-\log D(x; \psi)] + \frac{1}{2} \mathbb{E}^{z \sim \mathcal{N}} [-\log (1 - D(G(z; \theta); \psi))], \quad (6)$$

$$\mathcal{L}^{(G)} = \mathbb{E}^{z \sim \mathcal{N}} [-\log D(G(z; \theta); \psi)]. \quad (7)$$

The discriminator loss  $\mathcal{L}^{(D)}$  trains  $D$  to correctly classify real samples (maximizing  $\log D(x)$ ) and generated samples (maximizing  $\log(1 - D(G(z)))$ ). The generator loss  $\mathcal{L}^{(G)}$  trains  $G$  to produce samples that fool the discriminator (maximizing  $\log D(G(z))$ , equivalently minimizing  $-\log D(G(z))$ ).

The key advantage of per cluster training is that each GAN learns a unimodal distribution within its cluster rather than a complex mixture. This decomposition directly addresses mode collapse: when a single generator faces multiple distinct patterns, adversarial gradients become inconsistent as the discriminator penalizes outputs that deviate from any mode. By isolating behavioral patterns, each generator receives stable gradients pointing toward a coherent target distribution. This also ensures that rare operational modes receive dedicated modeling capacity rather than being overshadowed by dominant patterns.

Both networks are optimized by Adam with step size  $\eta$  and moments  $(\beta^{(1)}, \beta^{(2)})$ .

### 3.4. Continuous Device Generation

Continuous devices produce extended time series with gradual variations and long range temporal dependencies, requiring architectures capable of modeling sequential structure. The clustering procedure follows the same methodology as intermittent devices (Equations 4 and 5), as even devices with high occupancy exhibit multiple operational modes. Experimental validation confirms that continuous devices achieve silhouette scores above 0.8 with  $K \in \{6, 10\}$ , justifying universal application of cluster aggregation while using the continuous/intermittent classification to select appropriate generator architectures.

The primary challenge with continuous devices is sequence length. Raw traces may contain hundreds of thousands of samples, far exceeding what standard neural networks can process efficiently. Training a GAN directly on such long sequences leads to vanishing gradients, memory constraints, and unstable optimization. To address this, we apply uniform averaging with factor  $F \geq 1$  to create a simplified surrogate sequence  $\hat{x}$ :

$$\hat{x}_i = \frac{1}{F} \sum_{t=(i-1)F+1}^{iF} x_t, \quad i = 1: \left\lfloor \frac{T}{F} \right\rfloor. \quad (8)$$

This downsampling reduces the sequence by factor  $F$  while preserving low frequency components. When the simplified sequence still exceeds  $U = 1000$  samples, overlapping windows partition the data into manageable chunks.

**LSTM-GAN Architecture.** The generator maps a latent vector  $z \sim \mathcal{N}(0, I)$  through an affine layer, stacked LSTM layers, and a tanh output to produce bounded sequences in  $[-1, 1]$ . The discriminator processes input sequences through LSTM layers and extracts the final hidden state for binary classification. The LSTM architecture captures long range dependencies essential for modeling periodic patterns in continuous devices.

**Reconstruction.** After generation, the surrogate outputs  $\hat{y}$  must be mapped back to the original temporal resolution. This is achieved through block replication:

$$\text{Recon}(\hat{y}, F) = \left( \underbrace{\hat{y}_1, \dots, \hat{y}_1}_F, \dots, \underbrace{\hat{y}_n, \dots, \hat{y}_n}_F \right) \Big|_{1:T}, \quad (9)$$

with cropping or padding to achieve length  $T$ . This piecewise constant reconstruction preserves temporal structure while restoring the original sampling rate.

**Shared Adversarial Training.** CAG uses a shared discriminator  $D$  across all generated outputs (Figure 2). This design provides a unified quality standard that prevents individual branches from degrading without penalty, stabilizes adversarial dynamics by pooling gradient information across branches, and improves sample efficiency by learning transferable features of realistic power consumption. The shared discriminator is trained on the combined loss across all branches. Optimization uses Adam with step size  $\eta$  and moments  $(\beta^{(1)}, \beta^{(2)})$ .

**Hybrid Strategy for Complex Continuous Devices.** An alternative variant further distinguishes continuous devices into subcategories based on their waveform characteristics. Specifically, we identify square wave devices that exhibit on and off behavior with transitions and spiky devices that show irregular transients superimposed on a baseline.

A square wave pattern is detected when a 2 means clustering fit on a downsampled version of  $x$  yields cluster centers  $\{m_1, m_2\}$  satisfying:

$$|m_1 - m_2| > \gamma \text{std}(x), \quad (10)$$

where  $\gamma > 0$  is a separation factor. This condition checks whether the device operates in two distinct power states with sufficient separation relative to overall variability. Devices like simple on and off appliances such as kettles and toasters satisfy this criterion, while devices with continuous modulation such as variable speed motors and dimmable lights do not.

For square-wave devices, a transposed convolutional generator replaces the fully-connected architecture to better capture the sharp transitions characteristic of bistable behavior. The cycle length (duration of on/off periods) is estimated through transition analysis to set an appropriate segment length that captures complete cycles.

For spiky devices (those failing the square-wave test), salient events are extracted by peak finding at a quantile threshold:

$$\vartheta := \text{Quantile}_q(\{x_t : x_t > 0\}), \quad (11)$$

with  $q \in (0, 1)$  controlling the sensitivity. Samples exceeding  $\vartheta$  are identified as spike events, and surrounding windows of length  $S$  are extracted for training. Full length sequences are then reconstructed by stochastically interleaving generated spikes according to the empirically observed average spacing between peaks. This approach preserves the statistical properties of spike timing while allowing the generator to focus on producing realistic spike shapes.

---

#### Algorithm 1 Adaptive training pipeline

---

```

1: Load UVIC dataset and split by device
2: for each device do
3:   Detect type: continuous vs. intermittent
4:   if intermittent then
5:     Segment into windows
6:     Cluster windows into  $K$  patterns
7:     for each cluster do
8:       Train FC-GAN on segment vectors
9:     end for
10:  else
11:    Simplify long sequence
12:    Train LSTM-GAN on simplified series
13:  end if
14:  Save generators, losses, comparisons, and pattern visualizations
15: end for

```

---

## 4. Experiments

### 4.1. Dataset

The experimental data used in this paper comes from the UVIC Dataset, which collects time series data on appliance power consumption from real world residential and office environments. We cover a wide range of representative home

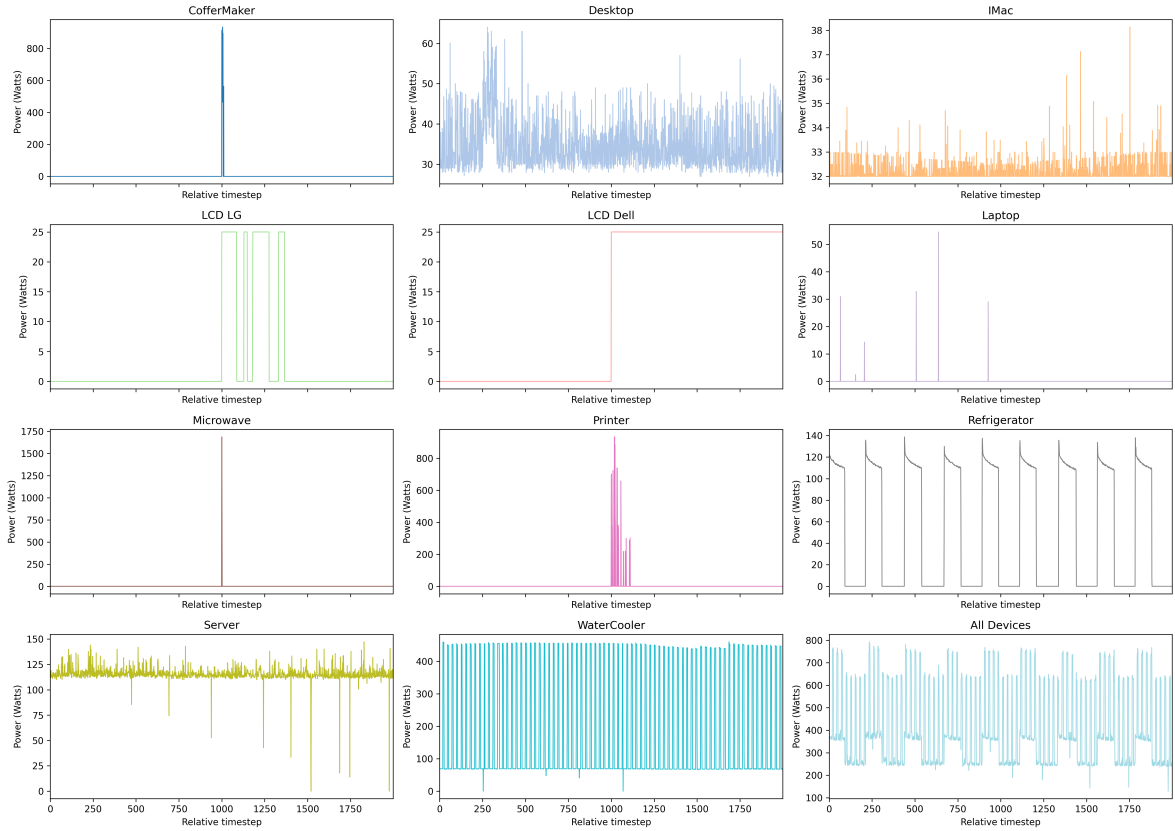


**Figure 3:** Visualization of appliance load profiles in the dataset. Representative time series power consumption patterns for multiple household and office appliances from the UVIC dataset. Each subplot shows the active power over time for a specific device, illustrating the diversity of load behaviors across appliance types. Intermittent devices such as the CoffeeMaker, Microwave, and Printer exhibit short, sporadic activations, whereas continuous devices such as the Desktop, IMac, Server, and Refrigerator display long duration, smoothly varying consumption trajectories. The variability in temporal structure and amplitude highlights the heterogeneity that motivates behavior based generative modeling in the proposed CAG framework.

appliances and electronic devices. The visualization can be found in Figure 3. This data records the active power variations of individual appliances in a time series format, offering high temporal resolution and behavioral diversity, fully reflecting the dynamic characteristics of different types of devices in daily use. The devices in the dataset include both continuous loads such as desktops, iMacs, servers, and refrigerators, whose power curves exhibit smooth and sustained trends, and intermittent loads such as coffee makers, microwaves, printers, and water coolers, which exhibit typical bursts and mode switching.

The raw data underwent a series of preprocessing to ensure quality and consistency. The UVIC dataset covers eleven categories of electrical appliances, demonstrating high representativeness and broad application potential. Its rich behavioral diversity provides a solid experimental foundation for synthetic data generation and non intrusive load monitoring (NILM) research. Through training and validation on this dataset, the model not only approximates the true power distribution in terms of statistical characteristics, but also maintains a high degree of similarity in structural and dynamic characteristics, providing reliable data support for energy consumption behavior modeling, data augmentation, and privacy protection.

## 4.2. Experimental settings

Table 1 summarizes the hyperparameters for both branches. Intermittent devices use segment length  $L = 436$  with Conv1D based generators and discriminators. Continuous devices are downsampled to at most 1000 points and modeled by two layer LSTM GANs. Both branches share Adam optimization with learning rate  $2 \times 10^{-4}$ ,  $\beta_1 = 0.5$ ,

**Table 1**

Core hyperparameters of the Cluster Aggregation GAN pipeline.

Intermittent branch	
Segment length $L$	436
Latent dimension $d_z$	100
Generator architecture	Conv1D(64, kernel=3) → Conv1D(128, kernel=5) → Conv1D(256, kernel=5) → Flatten → Linear( $L$ ), ReLU
Discriminator architecture	Conv1D(128, kernel=5) → Conv1D(64, kernel=3) → Flatten → Linear(1), LeakyReLU, Sigmoid
Epochs	1500
Batch size	32
Optimiser	Adam( $\eta = 2 \times 10^{-4}$ , $\beta_1 = 0.5$ , $\beta_2 = 0.999$ )
Loss	Binary cross entropy
Continuous branch	
Simplified horizon	$\leq 1000$ points (windows of 2000 when longer)
Latent dimension $d_z$	100
Generator	LSTM
Discriminator	LSTM
Epochs	1500
Batch size	32
Optimiser	Adam( $\eta = 2 \times 10^{-4}$ , $\beta_1 = 0.5$ , $\beta_2 = 0.999$ )
Loss	Binary cross entropy
Reconstruction	Repeat factor from Eq. (8)

$\beta_2 = 0.999$ , batch size 32, and 1500 training epochs. Classification thresholds are set to  $T_0 = 100$ ,  $\rho = 0.7$ , and  $\tau = 0.1$  following Eq. 2.

### 4.3. Evaluation Metrics

We benchmark all models with a set of domain specific metrics that jointly capture realism, diversity, and periodicity of appliance load curves. These two viewpoints mirror the goals of practical NILM and data synthesis: (1) Realism: generated traces must align with real power levels. (2) Diversity: cover the variety of user behaviours. Table 2 summarises the average metrics over all devices. Table 3 provides a detailed measurement from all devices. The first column enumerates the model identities, whereas the remaining columns correspond to quantitative indicators grouped by the above dimensions. To measure the metrics for realism, let  $\mathcal{X}_r = \{x^{(r)}\}$  and  $\mathcal{X}_g = \{x^{(g)}\}$  denote real and generated sequences with length  $T$ . We also denote empirical means and standard deviations by  $(\mu_r, \sigma_r)$  and  $(\mu_g, \sigma_g)$  respectively, and write  $\Phi(\cdot)$  for the feature extractor used in the Fréchet distance. Lower values imply closer waveform alignment and higher perceptual realism. The metrics are defined as follows.

**Mean Error (ME).** We compare first order statistics of real and generated signals

$$\text{ME} = \left| \mu_g - \mu_r \right|.$$

Smaller values indicate the generated sequences match the average power demand of the original appliance trajectories. This metric is the clearest indicator of whether the generator has recovered the long term energy budget of a device; large deviations imply that downstream NILM models would consistently over or under estimate consumption even if the temporal structure looked plausible.

**Standard Deviation Error (Std).** Second order consistency is measured through

$$\text{Std} = \left| \sigma_g - \sigma_r \right|.$$

Low deviation implies the synthetic signals reproduce the fluctuation intensity of the real series. Whereas ME focuses on the baseline level, the standard deviation reflects variability; it determines whether intermittent devices exhibit the correct amplitude contrast and whether continuous appliances retain natural drift rather than appearing overly smooth.

**Fidelity RMSE (Fid.).** Local waveform similarity is evaluated by matching each generated trace to its closest real neighbour:

$$\text{Fid.} = \frac{1}{|\mathcal{X}_g|} \sum_{x^{(g)} \in \mathcal{X}_g} \min_{x^{(r)} \in \mathcal{X}_r} \sqrt{\frac{1}{T} \|x^{(g)} - x^{(r)}\|_2^2}.$$

This root mean square error captures pointwise fidelity beyond the low order statistics above. A model with the right mean and variance can still miss transient ramps or spikes; the fidelity term penalises such shape discrepancies and therefore reflects how realistic an individual cycle will appear to a NILM classifier that utilizes detailed waveform cues.

**Period MAE (Per).** We estimate the dominant period  $\tau$  of each sequence via spectral peak detection and measure the mean absolute error

$$\text{Period} = \frac{1}{|\mathcal{X}_g|} \sum_{x^{(g)} \in \mathcal{X}_g} \left| \tau(x^{(g)}) - \tau(x_{\text{match}}^{(r)}) \right|,$$

where  $x_{\text{match}}^{(r)}$  is the closest real sequence in the sense of dominant frequency. Lower scores signify better preservation of appliance duty cycles. Period accuracy is critical for thermostatically controlled and compressor based loads whose duty cycle timing encodes operational behaviour. By keeping this error small we ensure that generated traces respect on/off cadence and rest intervals, which would otherwise break the plausibility of synthetic datasets despite matching instantaneous amplitudes.

**Feature FID (Fea).** Structural similarity in a learned feature space is measured through a Fréchet distance

$$\text{Fea} = \left\| m_r - m_g \right\|_2^2 + \text{Tr} \left( C_r + C_g - 2(C_r^{1/2} C_g C_r^{1/2})^{1/2} \right),$$

with  $(m_r, C_r)$  and  $(m_g, C_g)$  denoting the empirical mean and covariance of features  $\Phi(x^{(r)})$  and  $\Phi(x^{(g)})$ . Smaller values correspond to higher structural realism. Unlike the previous scalar statistics, the Feature FID evaluates high level embeddings learned from the entire waveform. It captures correlated variations such as typical ramp shapes or multi stage activation patterns. A low Feature FID therefore indicates that the generator reproduces latent appliance semantics beyond marginal distributions.

#### 4.3.1. Diversity Metrics

**Diversity RMSE (Div).** To ensure the generator does not collapse to a single pattern, we compute the average pairwise distance of generated samples

$$\text{Div} = \frac{2}{|\mathcal{X}_g|(|\mathcal{X}_g| - 1)} \sum_{i < j} \sqrt{\frac{1}{T} \|x_i^{(g)} - x_j^{(g)}\|_2^2}.$$

Moderately high values are desirable: too small indicates mode collapse, whereas excessively large values suggest unrealistic variability. This statistic quantifies whether the generator explores the full repertoire of usage patterns rather than collapsing to a single template.

**Cluster Coverage (CC).** Given  $K$  behavioural clusters extracted from real data, let  $n_k^{(g)}$  be the number of generated samples assigned to cluster  $k$ . Coverage is defined as

$$\text{Clus. Cov.} = \frac{1}{K} \sum_{k=1}^K \mathbf{1}[n_k^{(g)} > 0].$$

Values closer to 1 mean the generator reproduces all observed behavioural modes. This metric directly measures how many of the real world patterns survive in the synthetic dataset. A coverage gap implies some user behaviours disappear from training data, which would bias NILM models; maintaining high coverage ensures that even rare patterns (for example, late night microwave cycles) are synthesised.

**Cluster Jensen–Shannon Divergence (CJ).** Let  $p_r$  and  $p_g$  be the normalised cluster histograms for real and generated data. We compute

$$\text{CJ} = \frac{1}{2} \text{KL}(p_r \| m) + \frac{1}{2} \text{KL}(p_g \| m), \quad m = \frac{1}{2}(p_r + p_g),$$

where KL denotes the Kullback–Leibler divergence. Smaller values indicate balanced sampling across behavioural clusters.

While coverage checks whether every cluster appears at least once, the Jensen–Shannon divergence quantifies how closely the frequency of each patterns matches reality. Minimising CJ prevents the generator from over producing easy clusters and under representing difficult ones, yielding a synthetic corpus whose behavioural distribution mirrors the ground truth. Together these metrics reward models that simultaneously match real power, explore the behavioural space, and respect device periodicity, forming a comprehensive basis for the comparative studies in the following sections.

## 5. Result

### 5.1. Baselines

We benchmark CAG against four representative adversarial generators for time series: a CNN based GAN, an LSTM based GAN, an RNN based GAN, and a WaveGAN adapted for appliance traces. All baselines are trained on the UVIC dataset under identical data preprocessing, optimisation schedule, and sampling budgets, with hyperparameters tuned for stable convergence. This selection spans convolutional, recurrent, and waveform oriented inductive biases, providing a fair benchmark for assessing the routing and clustering design of CAG.

### 5.2. Overall comparison

Using the baselines described above, we compare CAG against CNN, LSTM, RNN, and waveform oriented GANs trained under identical UVIC settings. Table 2 reports average metrics across all devices, and Table 3 provides per device detail. Example outputs are shown in Figure 4.

Table 2 shows that CAG attains the best aggregate realism scores of mean error 8.03, standard deviation error 13.46, fidelity RMSE 42.6, period MAE 23.1, and Feature FID  $5.82 \times 10^{16}$  while simultaneously delivering the largest diversity metrics diversity RMSE  $1.34 \times 10^2$ , cluster coverage  $3.03 \times 10^{-1}$ , and cluster JS  $6.57 \times 10^{-1}$ . The closest baseline WaveGAN records a mean error of  $1.19 \times 10^2$ , and none of the alternatives approach CAG on coverage or balance, underscoring the benefit of treating clustering as part of the generator design rather than merely as a preprocessing aid.

The superior performance of CAG can be directly linked to its cluster aggregation strategy. By partitioning intermittent appliance signals into interpretable usage patterns and assigning an independent lightweight GAN to each cluster, the framework avoids the instability that often arises in monolithic adversarial models forced to learn highly multimodal distributions. This localized learning substantially reduces optimization variance and prevents mode collapse, leading to smoother convergence and lower generative bias. For continuous devices, the combination of sequence simplification and LSTM based temporal modeling further enhances stability by lowering the effective dimensionality of adversarial training and enabling the model to capture long range dependencies without gradient explosion or vanishing. Consequently, the quantitative outcomes in Table 2 not only demonstrate higher fidelity but also empirically confirm the theoretical convergence analysis described earlier.

The device statistics in Table 3 reinforce this trend. CAG captures the majority of realism metrics for continuous appliances such as Desktop, IMac, Server, and Refrigerator while retaining the top diversity indicators for every appliance. Isolated baseline wins do appear. CNN Base yields the lowest Desktop fidelity RMSE of 7.67 versus 8.68 and LSTM GAN tightens the CoffeeMaker standard deviation error to 9.46 versus 25.2. However, each comes with pronounced penalties elsewhere. Desktop mean error rises to  $1.31 \times 10^1$  versus  $9.61 \times 10^{-1}$  and CoffeeMaker mean error increases substantially to  $4.97 \times 10^2$  versus  $3.48 \times 10^1$ . Consequently, the cluster aggregated routing supplies the best overall balance between realism and pattern coverage.

The analysis of Table 2 and Table 3 corroborates the central claim of CAG framework achieves the best overall convergence and generalization performance, simultaneously ensuring statistical fidelity, behavioral diversity, and temporal stability. By integrating adaptive routing with cluster based adversarial training, CAG aligns its model capacity with the intrinsic heterogeneity of appliance behaviors, thereby establishing a robust and interpretable generative framework for synthetic load pattern generation.

### 5.3. Convergence analysis

To evaluate convergence stability, we trained CAG and the baselines under identical conditions. CAG achieves the fastest, smoothest, and most reliable convergence among all tested models (Figure 5). Its cluster based learning strategy and adaptive routing balance model capacity across heterogeneous appliances: intermittent traces are segmented into

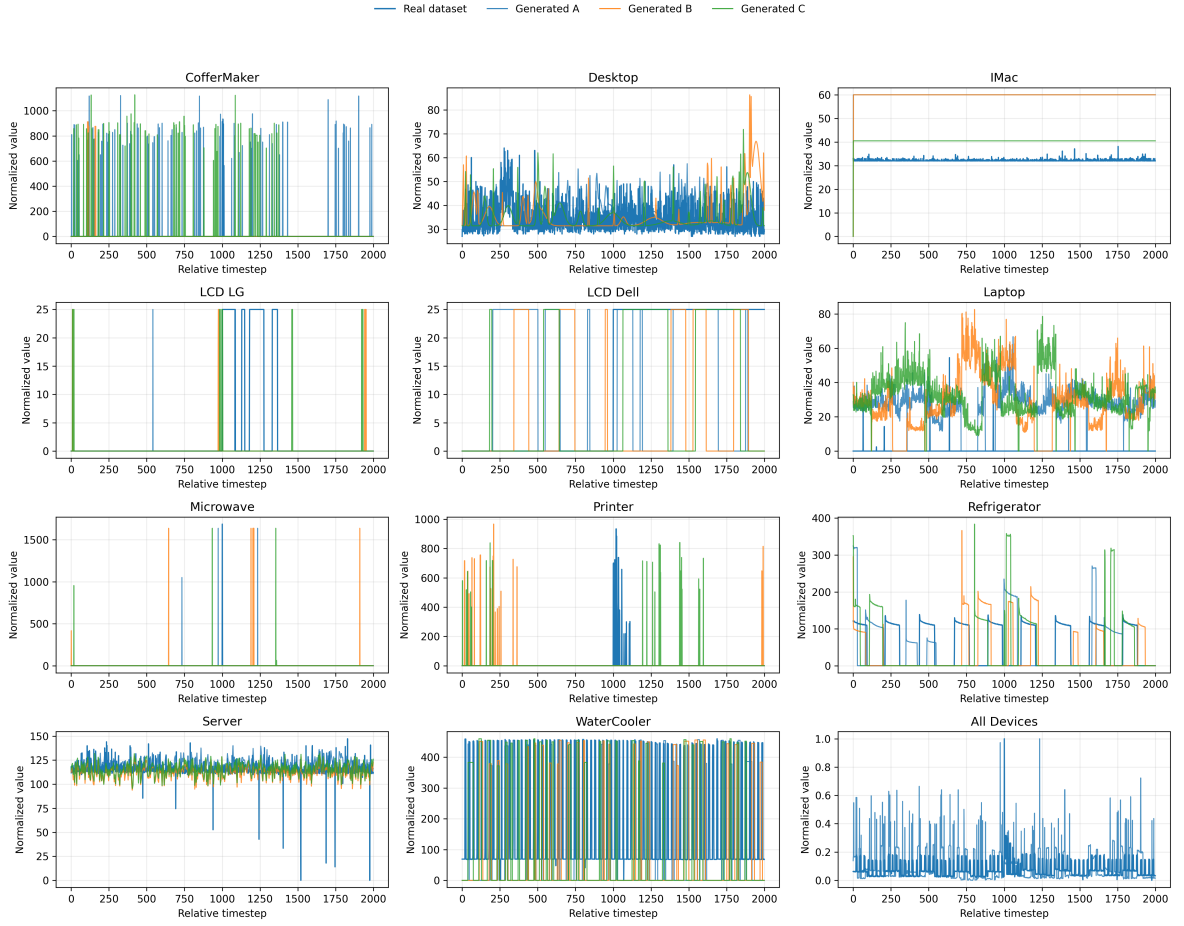


**Figure 4:** Example output visualization of the proposed CAG framework. The generated appliance load patterns closely resemble the real data, demonstrating the effectiveness of the cluster learning strategy and adaptive routing mechanism.

**Table 2**

Average realism and diversity metrics across all evaluated devices.

Model	Realism					Diversity		
	ME ↓	Std ↓	Fid ↓	Per ↓	Feature FID ↓	Div ↑	CC ↑	CJ ↑
CAG	$8.03e+00$ ▲	$1.35e+01$ ▲	$4.26e+01$ ▲	$2.31e+01$ ▲	$5.82e+16$ ▲	$1.34e+02$ ▲	$3.03e-01$ ▲	$6.57e-01$ ▲
CNN-Base	$1.20e+02$ ▼	$6.07e+01$ ▼	$1.39e+02$ ▼	$2.28e+02$ ▼	$9.97e+16$ ▼	$2.25e+01$ ▼	$8.58e-02$ ▼	$3.72e-01$ ▼
LSTM-GAN	$1.73e+02$ ▼	$1.91e+01$ ▼	$1.70e+02$ ▼	$1.91e+02$ ▼	$6.32e+16$ ▼	$6.14e+01$ ▼	$1.62e-01$ ▼	$3.70e-01$ ▼
RNN-GAN	$1.61e+02$ ▼	$7.92e+01$ ▼	$1.80e+02$ ▼	$2.37e+02$ ▼	$6.36e+16$ ▼	$1.22e+02$ ▼	$2.17e-01$ ▼	$3.66e-01$ ▼
WaveGAN	$1.19e+02$ ▼	$2.97e+01$ ▼	$1.24e+02$ ▼	$2.13e+02$ ▼	$6.40e+16$ ▼	$4.52e+01$ ▼	$1.41e-01$ ▼	$3.46e-01$ ▼

fixed length windows, transformed into shape based feature vectors, and modeled by lightweight GANs assigned to each cluster, which decomposes a multimodal problem into tractable subproblems. For continuous devices, the simplification reconstruction pipeline compresses redundant information via uniform averaging before LSTM based adversarial modeling, smoothing the optimisation landscape and mitigating exploding/vanishing gradients. Empirically, generator losses stabilize earlier and discriminator oscillations remain bounded, yielding the lowest mean error, standard deviation error, reconstruction RMSE, and Feature FID across devices.

The superior convergence of CAG arises from this cluster aggregation strategy, which reduces computational complexity, enhances feature specialization, and aligns model structure with the intrinsic heterogeneity of appliance behaviors. By decomposing complex temporal distributions into interpretable pattern clusters and assigning tailored

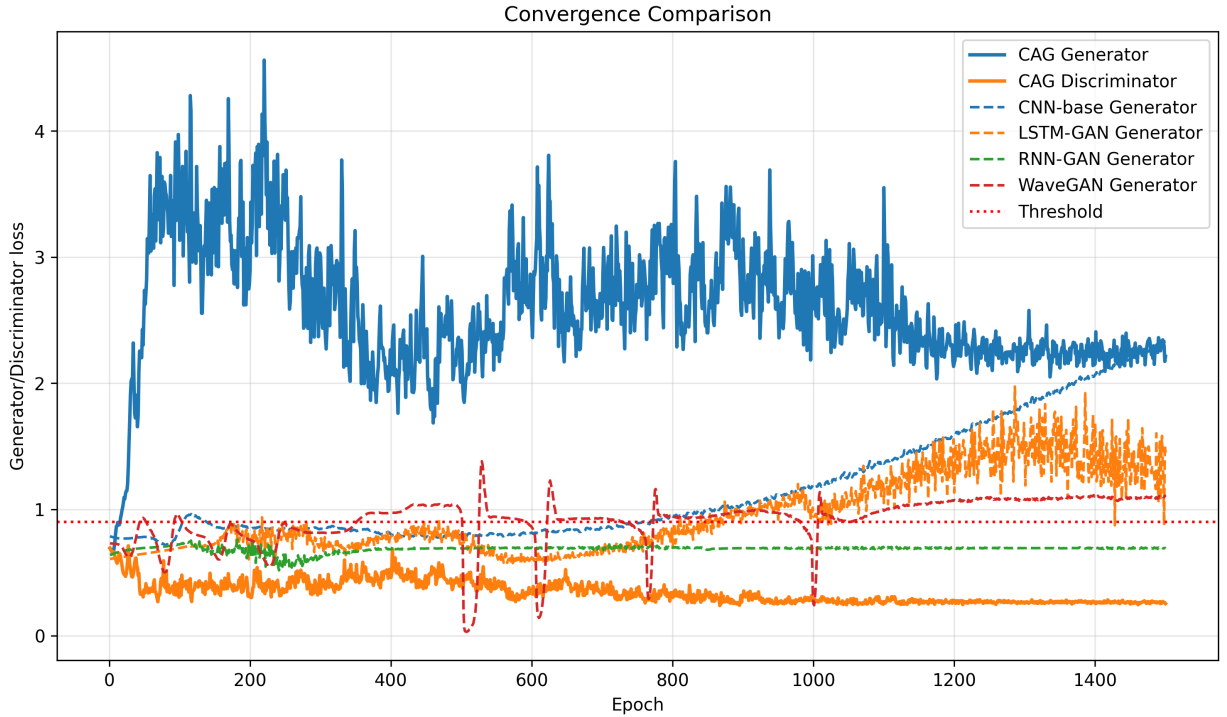


**Figure 5:** Convergence comparison of different generative models. The proposed CAG framework exhibits the most stable and consistent convergence behavior, with the generator and discriminator losses gradually approaching equilibrium. In contrast, baseline models such as CNN-base, LSTM-GAN, RNN-GAN, and WaveGAN show larger oscillations or divergence trends, indicating training instability. This demonstrates that the adaptive routing and clustering mechanisms in CAG effectively enhance training stability and improve convergence efficiency.

GANs to each, CAG attains a well regularized optimisation process that converges efficiently, stably, and with higher fidelity to actual energy consumption patterns.

#### 5.4. Cluster strategy verification

To verify that the heuristic routing used during training pairs each appliance with a suitable clustering strategy, we performed an auxiliary sweep using the full UVIC dataset. Each appliance column was segmented into 436 sample windows, normalized, and mapped to the shape based feature vector defined in Eq. 4. We then compared two strategies per device: (i) the deterministic continuous split that separates zero and nonzero windows, and (ii) a K Means clustering sweep with  $K \in \{2, 3, 4, 5, 6, 8, 10\}$ . For every  $K$  we computed the silhouette score to quantify coherence within clusters versus separation between clusters. This experiment replicates the statistics used inside the training loop but evaluates them offline, producing reproducible CSV summaries and per device silhouette curves.

Table 4 reports the detected appliance type, the winning strategy, and the best cluster count. Every device favored the K-Means path, even those whose sparsity statistics labeled them as continuous. Empirically, continuous loads also benefit from clustering because rare transients break the perfect two mode assumption behind the zero/non-zero split. High sparsity appliances such as LCD screens and printers preferred larger  $K$  values from 6 to 10 with silhouettes above 0.8, while continuously operating equipment such as desktops and servers peaked at  $K = 2$ . The low yet positive silhouette score for the aggregate channel indicates that this channel remains more heterogeneous than individual appliances, thus requiring careful handling by clustered GANs. These results justify using the clustered branch for all appliances while keeping the continuous and intermittent labels to decide generator architecture and reconstruction logic.

## 5.5. Ablation Study

To gauge the effect of the clustering stage alone, we retrained the CAG generator after disabling cluster aggregation for four representative appliances with two intermittent and two continuous. For each device we keep the rest of the pipeline unchanged and reuse the same hyperparameters and sampling budget as the clustered model. Table 5 contrasts the clustered as default and non clustered variants across the metrics introduced earlier.

Across all four devices the ablation confirms that clustering is the critical component for maintaining both realism and diversity. For CoffeeMaker, disabling clustering increases the mean error from  $3.48 \times 10^1$  to  $5.57 \times 10^2$  and the fidelity RMSE from  $1.32 \times 10^2$  to  $5.52 \times 10^2$  while cluster coverage collapses from  $4.94 \times 10^{-1}$  to  $1.67 \times 10^{-1}$ . Desktop exhibits a similar trend: period MAE nearly doubles from 8.45 to 16.1, Feature FID rises from  $8.61 \times 10^{11}$  to  $9.16 \times 10^{11}$ , and diversity RMSE shrinks from  $1.35 \times 10^1$  to 1.66. The long horizon Microwave improvements are particularly notable: fidelity RMSE is reduced by more than an order of magnitude from  $8.37 \times 10^2$  to  $6.45 \times 10^1$  and cluster coverage leaps from  $5.56 \times 10^{-2}$  to  $3.28 \times 10^{-1}$ . Water Cooler exhibits similar improvements with mean error decreasing from  $1.11 \times 10^2$  to  $1.22 \times 10^1$ , period MAE falling from  $5.57 \times 10^1$  to  $1.79 \times 10^1$ , and cluster JS improving from  $3.10 \times 10^{-1}$  to  $6.45 \times 10^{-1}$ . Together these results demonstrate that the clustering branch is essential: it prevents the generator from collapsing onto a limited set of modes and accounts for the substantial reductions in reconstruction error and the significant gains in coverage reported in Table 5.

**Table 3**  
Realism and diversity metrics for each device and model.

Device	Model	Realism					Diversity		
		ME ↓	Std ↓	Fid ↓	Per ↓	Feature FID ↓	Div ↑	CC ↑	CJ ↑
Coffee Maker	CAG	3.48e + 01▲	2.52e + 01▼	1.32e + 02▲	4.10e + 00▲	2.61e + 16▼	3.22e + 02▲	4.94e - 01▲	6.80e - 01▲
	CNN-Base	3.81e + 02▼	3.41e + 02▼	5.73e + 02▼	5.37e + 00▼	4.37e + 17▼	1.12e + 02▼	1.11e - 01▼	3.90e - 01▼
	LSTM-GAN	4.97e + 02▼	9.46e + 00▲	4.93e + 02▼	3.20e + 02▼	2.90e + 16▼	1.24e + 02▼	1.67e - 01▼	3.70e - 01▼
	RNN-GAN	3.58e + 02▼	1.69e + 02▼	3.75e + 02▼	3.00e + 02▼	2.90e + 16▼	3.06e + 02▼	4.44e - 01▼	3.60e - 01▼
	WaveGAN	3.59e + 02▼	1.09e + 01▼	3.59e + 02▼	9.24e + 01▼	1.79e + 16▲	1.30e + 02▼	1.67e - 01▼	3.20e - 01▼
Desktop	CAG	9.61e - 01▲	1.03e + 00▲	8.68e + 00▼	8.45e + 00▲	8.61e + 11▲	1.35e + 01▲	1.61e - 01▲	6.50e - 01▲
	CNN-Base	2.00e + 00▼	2.37e + 00▼	7.67e + 00▲	1.25e + 01▼	9.07e + 11▼	1.66e + 00▼	1.11e - 01▼	5.00e - 01▼
	LSTM-GAN	1.31e + 01▼	4.40e + 00▼	9.73e + 00▼	3.16e + 02▼	1.00e + 12▼	4.36e + 00▼	1.11e - 01▼	4.80e - 01▼
	RNN-GAN	1.07e + 01▼	2.20e + 00▼	9.37e + 00▼	2.73e + 02▼	1.00e + 12▼	1.19e + 01▼	5.56e - 02▼	4.30e - 01▼
	WaveGAN	1.47e + 01▼	7.29e + 00▼	1.00e + 01▼	3.83e + 01▼	9.97e + 11▼	1.28e + 00▼	5.56e - 02▼	4.20e - 01▼
iMac	CAG	4.20e - 01▲	5.93e - 01▲	1.79e + 00▲	4.15e + 01▲	6.69e + 11▼	1.77e + 02▲	3.83e - 01▲	6.40e - 01▲
	CNN-Base	5.59e - 01▼	2.01e + 00▼	4.36e + 00▼	9.27e + 01▼	6.83e + 11▼	2.82e - 01▼	5.56e - 02▼	4.60e - 01▼
	LSTM-GAN	9.11e - 01▼	1.06e + 00▼	2.57e + 00▼	3.47e + 02▼	7.20e + 11▼	3.90e + 00▼	3.33e - 01▼	4.40e - 01▼
	RNN-GAN	2.46e + 02▼	2.28e + 02▼	3.35e + 02▼	4.27e + 02▼	5.12e + 11▲	1.68e + 02▼	5.56e - 02▼	4.50e - 01▼
	WaveGAN	2.31e + 01▼	7.35e - 01▼	2.26e + 01▼	1.17e + 02▼	6.48e + 11▼	3.77e + 00▼	2.22e - 01▼	4.30e - 01▼
LCD-LG	CAG	4.34e - 02▲	9.77e - 01▼	1.73e + 00▲	4.78e + 01▲	1.55e + 12▼	6.34e + 00▲	1.06e - 01▲	6.30e - 01▲
	CNN-Base	2.29e + 00▼	1.49e + 00▼	2.84e + 00▼	4.33e + 02▼	1.55e + 12▼	3.21e - 01▼	5.56e - 02▼	4.20e - 01▼
	LSTM-GAN	9.03e + 00▼	3.94e - 01▼	9.26e + 00▼	9.71e + 01▼	1.55e + 12▼	2.61e + 00▼	5.56e - 02▼	4.00e - 01▼
	RNN-GAN	8.60e + 00▼	1.76e + 00▼	8.44e + 00▼	1.67e + 02▼	1.55e + 12▼	5.09e + 00▼	5.56e - 02▼	4.10e - 01▼
	WaveGAN	7.66e + 00▼	2.08e - 01▼	7.66e + 00▼	2.95e + 02▼	1.48e + 12▲	2.81e + 00▼	5.56e - 02▼	3.90e - 01▼
LCD-Dell	CAG	7.04e + 00▲	1.07e + 01▼	9.49e - 01▲	5.00e - 03▼	3.53e + 12▼	9.96e + 01▲	2.17e - 01▲	6.35e - 01▲
	CNN-Base	9.94e + 00▼	9.46e + 00▼	3.09e + 00▼	4.21e + 02▼	3.51e + 12▼	9.40e - 01▼	5.56e - 02▼	4.10e - 01▼
	LSTM-GAN	9.25e + 00▼	3.98e + 00▲	6.38e + 00▼	7.89e + 00▼	3.49e + 12▼	8.60e + 00▼	1.67e - 01▼	4.00e - 01▼
	RNN-GAN	6.01e + 01▼	9.11e + 01▼	1.04e + 02▼	0.00e + 00▲	3.03e + 12▲	9.39e + 01▼	1.67e - 01▼	3.90e - 01▼
	WaveGAN	3.33e + 01▼	6.92e + 00▼	2.60e + 01▼	3.06e + 02▼	3.17e + 12▼	5.28e + 00▼	1.11e - 01▼	3.80e - 01▼
Laptop	CAG	1.03e + 00▲	1.10e + 01▼	1.04e + 01▼	5.26e + 01▲	2.83e + 14▼	2.28e + 01▲	5.50e - 01▲	6.60e - 01▲
	CNN-Base	2.67e + 01▼	1.60e + 01▼	1.46e + 01▼	3.88e + 02▼	2.86e + 14▼	4.27e + 00▼	5.56e - 02▼	3.30e - 01▼
	LSTM-GAN	1.77e + 01▼	1.37e + 01▼	6.57e + 00▲	7.82e + 01▼	2.88e + 14▼	8.28e + 00▼	3.33e - 01▼	3.40e - 01▼
	RNN-GAN	1.77e + 01▼	2.86e + 00▲	6.67e + 00▼	2.69e + 02▼	2.88e + 14▼	2.08e + 01▼	5.00e - 01▼	3.50e - 01▼
	WaveGAN	3.41e + 01▼	1.36e + 01▼	2.21e + 01▼	3.52e + 02▼	2.77e + 14▲	8.57e + 00▼	2.78e - 01▼	3.20e - 01▼
Microwave	CAG	1.18e + 01▲	7.94e + 00▲	6.45e + 01▲	3.87e + 01▲	5.43e + 16▲	3.23e + 02▲	3.28e - 01▲	6.90e - 01▲
	CNN-Base	3.80e + 02▼	9.73e + 01▼	4.12e + 02▼	4.10e + 02▼	5.65e + 16▼	3.90e + 01▼	5.56e - 02▼	3.10e - 01▼
	LSTM-GAN	6.27e + 02▼	9.21e + 01▼	6.26e + 02▼	6.90e + 01▼	5.51e + 16▼	1.86e + 02▼	1.11e - 01▼	3.20e - 01▼
	RNN-GAN	6.34e + 02▼	1.99e + 02▼	6.30e + 02▼	2.40e + 02▼	5.52e + 16▼	3.07e + 02▼	2.78e - 01▼	3.30e - 01▼
	WaveGAN	6.61e + 02▼	1.07e + 02▼	6.74e + 02▼	3.30e + 02▼	7.58e + 16▼	2.08e + 02▼	1.11e - 01▼	3.00e - 01▼
Printer	CAG	1.67e + 01▼	1.05e + 01▲	6.41e + 01▼	3.34e + 01▲	1.74e + 15▲	1.99e + 02▲	3.83e - 01▲	6.70e - 01▲
	CNN-Base	2.48e + 02▼	5.73e + 01▼	2.66e + 02▼	4.27e + 02▼	2.36e + 15▼	4.92e + 01▼	5.56e - 02▼	3.20e - 01▼
	LSTM-GAN	4.61e + 02▼	4.20e + 01▼	4.55e + 02▼	9.62e + 01▼	2.71e + 15▼	1.05e + 02▼	1.11e - 01▼	3.30e - 01▼
	RNN-GAN	2.66e + 02▼	1.14e + 02▼	2.73e + 02▼	1.62e + 02▼	2.71e + 15▼	1.89e + 02▼	3.33e - 01▼	3.10e - 01▼
	WaveGAN	9.38e + 00▲	1.12e + 01▼	6.05e + 01▲	3.22e + 02▼	1.84e + 15▼	7.38e + 01▼	2.78e - 01▼	2.90e - 01▼
Refrigerator	CAG	2.48e + 00▲	1.01e + 01▼	5.72e + 01▲	0.00e + 00▲	4.23e + 16▲	8.07e + 01▲	2.17e - 01▲	6.55e - 01▲
	CNN-Base	6.37e + 01▼	4.34e + 01▼	7.01e + 01▼	2.22e + 02▼	6.84e + 16▼	1.08e + 01▼	1.11e - 01▼	3.00e - 01▼
	LSTM-GAN	1.24e + 02▼	3.00e + 01▼	8.67e + 01▼	7.55e + 01▼	6.91e + 16▼	3.81e + 01▼	1.67e - 01▼	3.20e - 01▼
	RNN-GAN	1.09e + 02▼	3.49e + 00▲	8.50e + 01▼	1.76e + 02▼	6.91e + 16▼	7.59e + 01▼	1.67e - 01▼	3.10e - 01▼
	WaveGAN	9.38e + 01▼	3.35e + 01▼	9.32e + 01▼	3.43e + 02▼	6.63e + 16▼	3.59e + 01▼	1.11e - 01▼	3.30e - 01▼
Server	CAG	8.75e - 01▲	3.27e + 00▼	1.21e + 01▲	9.15e + 00▲	1.88e + 11▲	3.81e + 01▲	3.28e - 01▲	6.75e - 01▲
	CNN-Base	1.05e + 00▼	8.02e + 00▼	1.68e + 01▼	3.32e + 01▼	8.12e + 11▼	4.51e + 00▼	2.22e - 01▼	3.40e - 01▼
	LSTM-GAN	3.04e + 01▼	5.71e + 00▼	2.91e + 01▼	3.37e + 02▼	2.78e + 11▼	1.64e + 01▼	1.11e - 01▼	3.50e - 01▼
	RNN-GAN	1.04e + 01▼	2.25e + 01▼	2.19e + 01▼	3.38e + 02▼	2.78e + 11▼	3.53e + 01▼	2.78e - 01▼	3.60e - 01▼
	WaveGAN	1.92e + 01▼	4.12e - 01▲	1.35e + 01▼	8.08e + 01▼	2.57e + 11▼	1.13e + 01▼	1.11e - 01▼	3.30e - 01▼
Water Cooler	CAG	1.22e + 01▲	6.67e + 01▼	1.15e + 02▼	1.79e + 01▲	5.16e + 17▲	1.88e + 02▲	1.61e - 01▲	6.45e - 01▲
	CNN-Base	2.04e + 02▼	8.95e + 01▼	1.62e + 02▼	6.00e + 01▼	5.32e + 17▼	2.49e + 01▼	5.56e - 02▼	3.10e - 01▼
	LSTM-GAN	1.18e + 02▼	7.63e + 00▲	1.49e + 02▼	3.57e + 02▼	5.39e + 17▼	1.78e + 02▼	1.11e - 01▼	3.20e - 01▼
	RNN-GAN	4.82e + 01▼	3.68e + 01▼	1.34e + 02▼	2.53e + 02▼	5.43e + 17▼	1.29e + 02▼	5.56e - 02▼	3.30e - 01▼
	WaveGAN	4.95e + 01▼	1.35e + 02▼	7.68e + 01▲	7.18e + 01▼	5.42e + 17▼	1.70e + 01▼	5.56e - 02▼	3.00e - 01▼

**Table 4**

Per device cluster strategy sweep. The recommended strategy is chosen by maximizing the silhouette score across the continuous split and K-Means candidates.

Device	Detected type	$K$	Silhouette
LCD_Dell	continuous	10	0.94
LCD-LG	continuous	6	0.96
CoffeeMaker	continuous	10	0.80
IMac	intermittent	2	0.28
Desktop	intermittent	2	0.27
Server	intermittent	2	0.13
WaterCooler	intermittent	2	0.15
Laptop	intermittent	10	0.58
Microwave	continuous	6	0.94
Printer	continuous	10	0.85
Refrigerator	intermittent	4	0.31

**Table 5**

Ablation results for removing cluster aggregation on four devices. Each metric follows the same Realism/Diversity grouping used in Tables 2 and 3.

Device	Variant	Realism					Diversity			
		ME ↓	Std ↓	Fid ↓	Per ↓	Feature FID ↓	Div ↑	CC ↑	CJ ↑	
Coffee Maker	With Clusters	$3.48e + 01$ ▲	$2.52e + 01$ ▲	$1.32e + 02$ ▲	$4.10e + 00$ ▲	$2.61e + 16$ ▲	$3.22e + 02$ ▲	$4.94e - 01$ ▲	$6.80e - 01$ ▲	
	No Clusters	$5.57e + 02$ ▼	$3.95e + 01$ ▼	$5.52e + 02$ ▼	$1.58e + 01$ ▼	$2.75e + 16$ ▼	$1.24e + 02$ ▼	$1.67e - 01$ ▼	$3.90e - 01$ ▼	
Desktop	With Clusters	$9.61e - 01$ ▲	$1.03e + 00$ ▲	$8.68e + 00$ ▲	$8.45e + 00$ ▲	$8.61e + 11$ ▲	$1.35e + 01$ ▲	$1.61e - 01$ ▲	$6.50e - 01$ ▲	
	No Clusters	$1.44e + 01$ ▼	$1.19e + 01$ ▼	$2.23e + 01$ ▼	$1.61e + 01$ ▼	$9.16e + 11$ ▼	$1.66e + 00$ ▼	$5.56e - 02$ ▼	$5.00e - 01$ ▼	
Microwave	With Clusters	$1.18e + 01$ ▲	$7.94e + 00$ ▲	$6.45e + 01$ ▲	$3.87e + 01$ ▲	$5.43e + 16$ ▲	$3.23e + 02$ ▲	$3.28e - 01$ ▲	$6.90e - 01$ ▲	
	No Clusters	$8.47e + 02$ ▼	$8.37e + 00$ ▼	$8.37e + 02$ ▼	$4.26e + 02$ ▼	$6.00e + 16$ ▼	$3.90e + 01$ ▼	$5.56e - 02$ ▼	$3.10e - 01$ ▼	
Water Cooler	With Clusters	$1.22e + 01$ ▲	$6.67e + 01$ ▲	$1.15e + 02$ ▲	$1.79e + 01$ ▲	$5.16e + 17$ ▲	$1.88e + 02$ ▲	$1.61e - 01$ ▲	$6.45e - 01$ ▲	
	No Clusters	$1.11e + 02$ ▼	$1.08e + 02$ ▼	$1.69e + 02$ ▼	$5.57e + 01$ ▼	$5.37e + 17$ ▼	$1.29e + 02$ ▼	$5.56e - 02$ ▼	$3.10e - 01$ ▼	

## 6. Conclusion

In this work, we presented Cluster Aggregated GAN (CAG), a pattern based generative framework designed to address the inherent heterogeneity of appliance patterns. By combining lightweight device classification, shape based segment clustering, and hybrid adversarial modeling, CAG aligns the generative process with the operational characteristics of intermittent and continuous devices. This design moves beyond conventional monolithic GAN architectures and enables conditioned learning, improved temporal stability, and interpretable synthetic pattern construction. Extensive experiments on the UVIC dataset demonstrate that CAG achieves superior realism, structural fidelity, and behavioral diversity compared with established baselines including CNN based GANs, LSTM GAN, RNN GAN, and WaveGAN. The proposed clustering mechanism proves essential for preventing mode collapse, enhancing motif coverage, and reducing reconstruction error, while the simplified LSTM branch stably models long duration continuous loads. Together, these components result in a balanced synthetic corpus with high fidelity that preserves both statistical properties and operational semantics of real appliance traces. Beyond performance gains, CAG provides a principled pathway for scalable and interpretable synthetic load generation in NILM research. By treating clustering as an integral generative component rather than a preprocessing step, the framework offers a generalizable paradigm for modeling complex multimodal time series data.

The limitations of this work are: quality depends on the chosen window length  $L$ ; training for each cluster increases compute when  $K$  grows; and handcrafted shape features may bias motif discovery. These open avenues for adaptive windowing, budget constrained clustering, and learned feature extractors. Future work will also explore conditioning on contextual factors such as occupancy, environment, or user routines, and extend CAG toward privacy preserving and cross dataset synthetic data generation.

## References

- [1] Adewole, K.S., Torra, V., 2023. Privacy protection of synthetic smart grid data simulated via generative adversarial networks, in: Proceedings of the 20th International Conference on Security and Cryptography (SECRYPT), pp. 279–286.
- [2] Angelis, G.F., et al., 2022. NILM applications: Literature review of learning approaches, recent developments and challenges. *Energy and Buildings* 261, 111951. doi:10.1016/j.enbuid.2022.111951.
- [3] Arjovsky, M., Chintala, S., Bottou, L., 2017. Wasserstein GAN, in: Proceedings of the 34th International Conference on Machine Learning (ICML), pp. 214–223.
- [4] Bashar, M.A., Nayak, R., 2023. Algan: Time series anomaly detection with adjusted- lstm gan. arXiv preprint arXiv:2308.06663 .
- [5] Batra, N., Kelly, J., Parson, O., Bergés, M., 2014. NILMTK: An open source toolkit for energy disaggregation, in: Proceedings of the 5th International Conference on Future Energy Systems (ACM e-Energy), pp. 265–276.
- [6] Bedi, G., Aujla, G.S., Tanwar, S., Kumar, R., Kumar, N., 2018. Review of internet of things in electric power and energy systems. *IEEE Internet of Things Journal* 5, 847–870. doi:10.1109/JIOT.2018.2802704.
- [7] Buneeva, N., Reinhardt, A., 2017. Ambal: Appliance modeling by aggregation of load segments, in: Proceedings of the 8th International Conference on Future Energy Systems (e-Energy), pp. 287–292.
- [8] Castangia, M., et al., 2025. Residential load modeling with generative adversarial networks. *IEEE Transactions on Sustainable Computing Early Access*.
- [9] Chen, D., Irwin, D., Shenoy, P., 2016. SmartSim: A device-accurate smart home simulator for energy analytics, in: Proceedings of the IEEE International Conference on Smart Grid Communications (SmartGridComm 2016), pp. 686–692.
- [10] El Kababji, S., Srikantha, P., 2020. A data-driven approach for generating synthetic load patterns and usage habits. *IEEE Transactions on Smart Grid* 11, 4984–4995.
- [11] Esteban, C., Hyland, S.L., Rättsch, G., 2017. Real-valued (medical) time series generation with recurrent conditional gans. arXiv preprint arXiv:1706.02633 .
- [12] Faustine, W., Suchithra, N., Mushi, L., et al., 2017. A survey on non-intrusive load monitoring. *Energies* 10, 957. doi:10.3390/en10070957.
- [13] Gkoutroumpi, C., Gkalinikis, N.V., Vrakas, D., 2024. SGAN: Appliance signatures data generation for NILM applications using GANs, in: Proceedings of the 12th Computing Conference (Science and Information Conference, SAI 2024), Springer. pp. 325–339. doi:10.1007/978-3-031-62269-4\_23.
- [14] Goodfellow, I., Pouget-Abadie, J., Mirza, M., Xu, B., Warde-Farley, D., Ozair, S., Courville, A., Bengio, Y., 2020. Generative adversarial networks. *Communications of the ACM* 63, 139–144.
- [15] Guo, Z., Adedigba, A.P., Mallipeddi, R., 2025a. Cluster-aggregated transformer: Enhancing lightweight parameter models. *Engineering Applications of Artificial Intelligence* 159, 111468. doi:10.1016/j.engappai.2025.111468.
- [16] Guo, Z., Adedigba, A.P., Mallipeddi, R., Lee, H., 2025b. Dynamic tanh reinforcement learning: A normalization-free transformer for open traveling salesman problem optimization. *Journal of the Institute of Control, Robotics and Systems Conference Proceedings* , 845–846.
- [17] Guo, Z., Kavuri, S., Lee, J., Lee, M., 2023. IDS-Extract: Downsizing deep learning model for question and answering, in: Proceedings of the 2023 International Conference on Electronics, Information, and Communication (ICEIC), pp. 1–5. doi:10.1109/ICEIC57457.2023.10049915.
- [18] Harell, A., Jones, R., Makonin, S., Bajic, I.V., 2021. TraceGAN: Synthesizing appliance power signatures using generative adversarial networks. *IEEE Transactions on Smart Grid* 12, 4553–4563. doi:10.1109/TSG.2021.3078695.

- [19] Hart, G.W., 1992. Nonintrusive appliance load monitoring. *Proceedings of the IEEE* 80, 1870–1891. doi:10.1109/5.192069.
- [20] Huang, F., Deng, Y., 2023. Tcgan: Convolutional generative adversarial network for time series classification and clustering. *Neural Networks* 165, 868–883.
- [21] Internò, C., et al., 2025. SIDED: Synthetic industrial dataset for energy disaggregation via digital twins. *arXiv preprint arXiv:2506.20525*. URL: <https://arxiv.org/abs/2506.20525>.
- [22] Jaradat, A., Al-Sareh, M., Al-Ghazo, S., et al., 2024. HYDROSAFE: A hybrid deterministic-probabilistic model for synthetic appliance profiles generation. *Sensors* 24, 5532. doi:10.3390/s24155532.
- [23] Kamyshev, I., Moghimian, S., Ouerdane, H., 2025. HiFAKES: Synthetic high-frequency NILM data for NILM models diagnostics and generalization testing. *arXiv preprint arXiv:2409.00062* URL: <https://arxiv.org/abs/2409.00062>.
- [24] Kelly, J., Knottenbelt, W., 2015. Neural NILM: Deep neural networks applied to energy disaggregation, in: *Proceedings of the 2nd ACM International Conference on Embedded Systems for Energy-Efficient Built Environments (BuildSys)*, pp. 55–64.
- [25] Kingma, D.P., Welling, M., 2014. Auto-encoding variational bayes, in: *Proceedings of the International Conference on Learning Representations (ICLR)*.
- [26] Klemenjak, C., Kovatsch, C., Herold, M., Elmenreich, W., 2020. SynD: A synthetic energy dataset for non-intrusive load monitoring in households. *Scientific Data* 7, 108. doi:10.1038/s41597-020-0434-6.
- [27] Liang, X., Wang, H., 2025. Learning and generating diverse residential load patterns using GAN with weakly-supervised training and weight selection. *IEEE Transactions on Consumer Electronics* 71, 2837–2848. doi:10.1109/TCE.2025.3563272.
- [28] Lin, Z., Han, J., Zhu, Q., et al., 2020. Using GANs for sharing networked time series data, in: *Proceedings of the ACM Internet Measurement Conference (IMC)*, pp. 464–481.
- [29] Meiser, M., Dümpe, B., Zinnikus, I., 2024. VA-creator: A virtual appliance creator based on adaptive neural networks to generate synthetic power consumption patterns. *Energy and AI* 8, 100205.
- [30] Mirza, M., Osindero, S., 2014. Conditional generative adversarial nets. *arXiv preprint arXiv:1411.1784*. URL: <https://arxiv.org/abs/1411.1784>.
- [31] Mukherjee, S., Asnani, H., Alfonzo, E., Kannan, S., 2019. ClusterGAN: Latent space clustering in generative adversarial networks, in: *Proceedings of the AAAI Conference on Artificial Intelligence*, pp. 4610–4617.
- [32] Nalmpantis, C., Vrakas, D., 2019. Machine learning approaches for non-intrusive load monitoring: from qualitative to quantitative comparison. *Artificial Intelligence Review* 52, 217–243. doi:10.1007/s10462-018-9650-2.
- [33] Odena, A., Olah, C., Shlens, J., 2017. Conditional image synthesis with auxiliary classifier GANs, in: *Proceedings of the 34th International Conference on Machine Learning (ICML)*, pp. 2642–2651.
- [34] Smith, K.E., Smith, A.O., 2020. Conditional GAN for time series generation. *arXiv preprint arXiv:2006.16477*. URL: <https://arxiv.org/abs/2006.16477>.
- [35] Sykiotis, S., Kaselimi, M., Doulamis, A., Doulamis, N., 2022. ELECTRICity: An efficient transformer for non-intrusive load monitoring. *Sensors* 22, 2926. doi:10.3390/s22082926.
- [36] Varanasi, L.S., Karri, S.P.K., 2023. STNILM: Switch transformer-based NILM adaptive to households. *Energy and Buildings* 275, 113249.
- [37] Wang, X., et al., 2021. DPP-GAN: A decentralized and privacy-preserving GAN system for collaborative smart meter data generation. *arXiv preprint arXiv:2110.12345*. URL: <https://arxiv.org/abs/2110.12345>.
- [38] Yang, M., Wang, Z., Chi, Z., Feng, W., 2022. Wavegan: Frequency-aware gan for high-fidelity few-shot image generation, in: *European conference on computer vision*, Springer. pp. 1–17.
- [39] Yoon, J., Jarrett, D., van der Schaar, M., 2019. Time-series generative adversarial networks, in: *Advances in Neural Information Processing Systems* 32 (NeurIPS 2019), pp. 5509–5519.
- [40] Zeifman, M., Roth, K., 2011. Nonintrusive appliance load monitoring: Review and outlook. *IEEE Transactions on Consumer Electronics* 57, 76–84. doi:10.1109/TCE.2011.5735484.